

Mitochondrial Dysfunction and Oxidative Damage in *parkin*-deficient Mice*

Received for publication, February 2, 2004, and in revised form, February 19, 2004
Published, JBC Papers in Press, February 24, 2004, DOI 10.1074/jbc.M401135200

James J. Palacino^{‡§}, Dijana Sagi[¶], Matthew S. Goldberg^{‡§}, Stefan Krauss^{||}, Claudia Motz^{||},
Maik Wacker^{||}, Joachim Klose^{||}, and Jie Shen^{‡**}

From the [‡]Center for Neurologic Diseases, Brigham and Women's Hospital and ^{||}Department of Endocrinology, Beth Israel Deaconess Medical Center, Harvard Medical School, Boston, Massachusetts 02115 and [¶]Institute for Human Genetics, University Clinic Charité, D-13353 Berlin, Germany

Loss-of-function mutations in *parkin* are the predominant cause of familial Parkinson's disease. We previously reported that *parkin*^{-/-} mice exhibit nigrostriatal deficits in the absence of nigral degeneration. *Parkin* has been shown to function as an E3 ubiquitin ligase. Loss of *parkin* function, therefore, has been hypothesized to cause nigral degeneration via an aberrant accumulation of its substrates. Here we employed a proteomic approach to determine whether loss of *parkin* function results in alterations in abundance and/or modification of proteins in the ventral midbrain of *parkin*^{-/-} mice. Two-dimensional gel electrophoresis followed by mass spectrometry revealed decreased abundance of a number of proteins involved in mitochondrial function or oxidative stress. Consistent with reductions in several subunits of complexes I and IV, functional assays showed reductions in respiratory capacity of striatal mitochondria isolated from *parkin*^{-/-} mice. Electron microscopic analysis revealed no gross morphological abnormalities in striatal mitochondria of *parkin*^{-/-} mice. In addition, *parkin*^{-/-} mice showed a delayed rate of weight gain, suggesting broader metabolic abnormalities. Accompanying these deficits in mitochondrial function, *parkin*^{-/-} mice also exhibited decreased levels of proteins involved in protection from oxidative stress. Consistent with these findings, *parkin*^{-/-} mice showed decreased serum antioxidant capacity and increased protein and lipid peroxidation. The combination of proteomic, genetic, and physiological analyses reveal an essential role for *parkin* in the regulation of mitochondrial function and provide the first direct evidence of mitochondrial dysfunction and oxidative damage in the absence of nigral degeneration in a genetic mouse model of Parkinson's disease.

Parkinson's disease (PD)¹ is the second most prevalent neurodegenerative disease. Clinical manifestations of PD include

* This work was supported by a Harvard Center for Neurodegeneration and Repair Translational Research Fellowship (to J. J. P.), by Bundesministerium fuer Bildung und Forschung (to D. S. and J. K.), and by grants from NINDS, National Institutes of Health (to J. S.). The costs of publication of this article were defrayed in part by the payment of page charges. This article must therefore be hereby marked "advertisement" in accordance with 18 U.S.C. Section 1734 solely to indicate this fact.

§ These authors contributed equally to this work.

** To whom correspondence should be addressed: Center for Neurologic Diseases, Harvard Medical School, New Research Bldg. 636E, 77 Avenue Louis Pasteur, Boston, MA 02115. Tel.: 617-525-5561; Fax: 617-525-5522; E-mail: jshen@rics.bwh.harvard.edu.

¹ The abbreviations used are: PD, Parkinson's disease; ROS, reactive oxygen species; 4HNE, 4-hydroxynonenal; DA, dopamine; DAT, dopa-

mine transporter; MS, mass spectrometry; pI, isoelectric point; TMPD, N,N,N',N'-tetramethylphenylenediamine; FCCP, carbonyl cyanide 4-(trifluoromethoxy)phenylhydrazone; PRDX, peroxiredoxin.

postural instability, bradykinesia, resting tremor, and rigidity. Neuropathologically, the disease is characterized by the selective degeneration of the dopaminergic neurons in the substantia nigra (1). The etiology of PD is still unknown, although clinical and experimental evidence implicate the involvement of mitochondrial dysfunction (2, 3) and oxidative stress (4, 5). Analysis of mitochondria isolated from idiopathic PD patients showed inhibited capacity of NADH-ubiquinone reductase, complex I of the mitochondrial electron transport chain, and increased production of reactive oxygen species (ROS) (6). Similar changes have been seen in autopsy cases of patients with presymptomatic PD, suggesting that mitochondrial dysfunction and oxidative stress precede clinical manifestations (7).

Exposure to selective neurotoxins, including paraquat and 1-methyl-4-phenyl-1,2,3,6-tetrahydropyridine (MPTP), has been linked to either increased risk of PD or chemically induced parkinsonism (8, 9). These compounds have been shown experimentally to decrease mitochondrial function and selectively inhibit the activity of complex I (10). *In vitro* chemical inhibition of complex I results in reduced oxidative phosphorylation and increased mitochondrial generation of ROS, similar to what was observed in mitochondria from PD patients (11–13). Pathological examinations of PD brains have revealed increases in protein and lipid byproducts of ROS, including protein carbonyls and 4-hydroxynonenal (4HNE) (14, 15). Furthermore, 4HNE forms adducts with and inhibits the activities of the D1 dopamine (DA) receptor and the DA transporter (DAT), suggesting that lipid peroxides may contribute to the disruption of DA signaling (16, 17). Cultured dopaminergic neurons have been shown to exhibit enhanced sensitivity to paraquat and MPTP (1-methyl-4-phenyl-1,2,3,6-tetrahydropyridine) as well as ROS (18). These findings suggest that mitochondrial dysfunction and accompanying ROS generation could be a common mechanism for the selective loss of substantia nigra neurons and the nigrostriatal DA signal in PD (19).

In addition to the more prevalent, idiopathic form, a subset of PD patients exhibits familial inheritance patterns. Large numbers and varieties of autosomal recessively inherited mutations in *parkin* are the predominant cause of familial PD (20). Initially described as juvenile-onset, atypical parkinsonism lacking Lewy bodies, subsequently identified cases are often clinically and pathologically indistinguishable from early onset familial or sporadic PD, including the presence of Lewy bodies in a single case (21–23). We have recently reported that the loss of *parkin* function in mice results in nigrostriatal dysfunction, as evidenced by increased extracellular dopamine concentra-

mine transporter; MS, mass spectrometry; pI, isoelectric point; TMPD, N,N,N',N'-tetramethylphenylenediamine; FCCP, carbonyl cyanide 4-(trifluoromethoxy)phenylhydrazone; PRDX, peroxiredoxin.

tion in the striatum, reduced synaptic excitability in the striatal neurons, and behavioral deficits in paradigms that are sensitive to alterations in the nigrostriatal pathway (24). Despite measurable differences in nigrostriatal function in *parkin*^{-/-} mice (24), no reduction in the number of dopaminergic neurons was observed in two independently generated *parkin*^{-/-} mice (24, 25).

Parkin has been reported as an E3 ubiquitin-protein ligase (26). Previous reports described several substrates for parkin-mediated ubiquitinylation (27). It has been suggested that the loss of parkin function results in aberrant accumulation of substrate proteins including PAEL receptor, synphlin-1, and CDC-rel1. Accumulation of one or more of these proteins has been postulated to confer toxicity upon dopaminergic neurons in the substantia nigra (28). However, steady-state levels of these substrates are unchanged in *parkin*^{-/-} brains (24).² Recent evidence has also suggested a role for parkin in the protection of monoaminergic neurons against proteasomal dysfunction, α -synuclein overexpression-mediated cell death (29), and kainic acid-induced toxicity (30). It was shown that parkin is localized in mitochondria and inhibits mitochondria-dependent cell death (31). Other studies demonstrate that overexpression of mutant parkin elevates cellular markers of oxidative stress, whereas overexpression of wild-type parkin results in reduced levels of these markers (32). These observations are consistent with findings from *parkin*-null flies, which exhibit altered mitochondrial morphology and degeneration of tissues such as wing flight muscles and spermatocytes (33). These results raised the possibility that parkin may be involved in mitochondrial function. Based on these observations, we hypothesized that lack of parkin function may cause impairment of mitochondrial function in *parkin*^{-/-} mice.

To determine whether a lack of parkin causes changes in protein abundance and/or modification, we conducted a nonbiased proteomic analysis of the ventral midbrain of *parkin*^{-/-} and wild-type mice. Using a well established method for two-dimensional analysis of brain lysates (34), we were able to detect ~8000 discrete protein spots from extracts of the ventral midbrain of *parkin*^{-/-} and wild-type mice. Comparative analysis of 10 pairs of wild-type and *parkin*^{-/-} brain samples revealed reproducible, quantitative changes of fifteen protein spots by silver staining. Subsequent mass spectrometric (MS) analysis revealed that these 15 spots represented 14 distinct proteins, 13 of which exhibited decreases in abundance in brains of *parkin*^{-/-} mice and 1 additional protein which exhibited altered electrophoretic mobility, consistent with differential post-translational modification. Eight of these proteins were involved in either oxidative phosphorylation or antioxidant activities. Consistent with these findings, *parkin*^{-/-} mice exhibited decreases in oxidative phosphorylation, weight gain, and antioxidant capacity as well as increased ROS-mediated tissue damage, suggesting an essential role for parkin in regulating normal respiratory function of mitochondria as well as in the protection of cells from oxidative stress.

MATERIALS AND METHODS

Mice—Mice bearing a germline disruption of exon 3 of the *parkin* gene were generated as previously described (24). Mice used for all studies except the proteomic analysis were in the hybrid background of C57BL/6 and 129/Sv. Mice used for proteomic studies were the 129/Sv inbred strain.

Two-dimensional Gel Electrophoresis and Mass Spectrometry—Protein samples for two-dimensional gel electrophoresis were prepared from the dissected ventral midbrain (including the substantia nigra) of each of the 10 pairs of *parkin*^{-/-} and wild-type mice as previously described (35) with the following modifications. The solutions used for

extractions were 100 mM phosphate buffer, pH 7.1 (0.2 M KCl, 20% w/v glycerol, and 4% w/v 3-[(3-chloramidopropyl) dimethylammonio]-1-propanesulfonate) (A), protease inhibitor solution I (1 Complete™ tablet (Roche Applied Science) dissolved in 2 ml of buffer A) (B), and protease inhibitor solution II (1.4 μ M pepstatin A and 1 mM phenylmethylsulfonyl fluoride in ethanol) (C). The frozen tissue was transferred into a mortar placed in a liquid nitrogen bath. An aliquot of 1.25 parts v/w of A, 0.08 parts v/w of protease inhibitor I, and 0.02 parts v/w of protease inhibitor II were added to the tissue and ground to a fine powder. The resulting powder was filled into a 2-ml microtube, quickly thawed, supplied with 0.034 parts of glass beads, and then sonicated in an ice-cold water bath 6 times for 10 s with intervals of 1 min 50 s. The homogenate was stirred 30 min in the presence of 0.025 parts v/w of Benzonase (Merck). 6.5 M urea, 2 M thiourea, and 70 mM dithiothreitol solution were added, and stirring was continued for an additional 30 min. The protein extract was supplied with 0.1 parts v/w of ampholyte mixture Servalyte pH 2–4 (Serva, Heidelberg, Germany) and stored at –80 °C or analyzed immediately.

Proteins were separated by large two-dimensional gels as described previously (34, 35). Briefly, the gel format was 40 cm (isoelectric focusing, prepared with carrier ampholyte mixture covering pH 3–10) \times 30 cm (SDS-PAGE, 15%) \times 0.75 mm. The amount of the protein sample applied to the gel was 5 μ l (60 μ g/ μ l). For sample comparisons brain extracts from each pair of *parkin*^{-/-} and control mice were run and stained in parallel. High sensitivity silver staining was used to visualize proteins (35). Two-dimensional gels were evaluated visually pairwise, and changes of spots were considered with respect to variation in the presence or absence, quantity, and spot position. Protein spots found to be reproducibly altered in *parkin*^{-/-} patterns versus wild type were evaluated with the Proteomweaver imaging software Version 2.1 (Definiens, Munich, Germany). Although the mice we used are in a homogenous genetic background (129/Sv inbred strain), we still observed individual variations. Protein alterations confirmed in more than six pairs of mice were scored. All 10 *parkin*^{-/-} mice investigated were affected at least in 7 of 14 proteins, and 5 mice were affected in more than 12 proteins. Data were analyzed by Student's *t* test.

For protein identification using MS, 18- μ l (60 μ g/ μ l) samples were electrophoresed on 1.5-mm gels and stained with MS-compatible silver stain or colloidal Coomassie Brilliant Blue G-250. Protein spots of interest were excised from gels and subjected to in-gel trypsin digestion without reduction or alkylation. Tryptic fragments were analyzed by a combination of matrix-assisted laser desorption/ionization time-of-flight and liquid chromatography/electrospray ionization ion trap MS. The mass spectra were analyzed using Protein Prospector (MS-Fit) and Sequest Version 3.1 software.

Mitochondrial Respiration—Mice were euthanized by CO₂ inhalation, and tissues were rapidly dissected on ice. Brains were removed, and striata were isolated as described previously (24). Striata from 2 mice of each genotype were pooled for mitochondrial isolation. Tissue samples were homogenized in 10 ml of buffer A (320 mM sucrose, 5 mM Tris, 2 mM EGTA, pH 7.4, at 4 °C) with 5 strokes of a Teflon Dounce. Samples were centrifuged for 3 min at 2000 \times *g* to remove nuclei and tissue particles. Supernatants were collected and centrifuged for 10 min at 12,000 \times *g* to pellet mitochondria and synaptosomes. The crude pellet was resuspended in 10 ml of buffer A with the addition of 0.02% w/v of digitonin to disrupt synaptosomal membranes and release trapped mitochondria. The resuspended pellet was centrifuged for 10 min at 12,000 \times *g* to pellet mitochondria, which was resuspended in 100 μ l of buffer A, and protein content was determined by BCA assay (Pierce). Mitochondria were resuspended at a final concentration of 0.4 mg/ml protein in 0.5 ml of buffer B (120 mM KCl, 3 mM HEPES, 1 mM EGTA, 5 mM KH₂PO₄, pH 7.2) with 1% w/v of bovine serum albumin and assayed for respiration using an excess of 8 mM glutamate, 8 mM malate (complex I), 4 mM succinate (complex II), or 0.4 mM N,N,N',N'-tetramethylphenylenediamine (TMPD)/1 mM ascorbate (complex III/IV) as electron donors. ADP was added in limiting amounts (14 μ M), and state 3 respiration was measured. After depletion of ADP, state 4 respiration was measured. After determination of coupled respiration, 400 nM carbonyl cyanide 4-(trifluoromethoxy)phenylhydrazone (FCCP) was added to the reaction chamber, and respiration was measured in the absence of a proton gradient. Mitochondrial respiration was determined using a platinum electrode with a 1-ml buffer chamber (DM-10, Rank Bros., Ltd., UK). Due to intra-day variations in respiration rates, oxygen consumption values are represented as a fraction of the wild-type state 3 respiration for succinate. Data were analyzed by unpaired Student's *t* test.

Electron Microscopy—Wild-type and *parkin*^{-/-} mice were euthanized by CO₂ inhalation and transcardially perfused with 20 ml of

² J. J. Palacino and J. Shen, unpublished results.

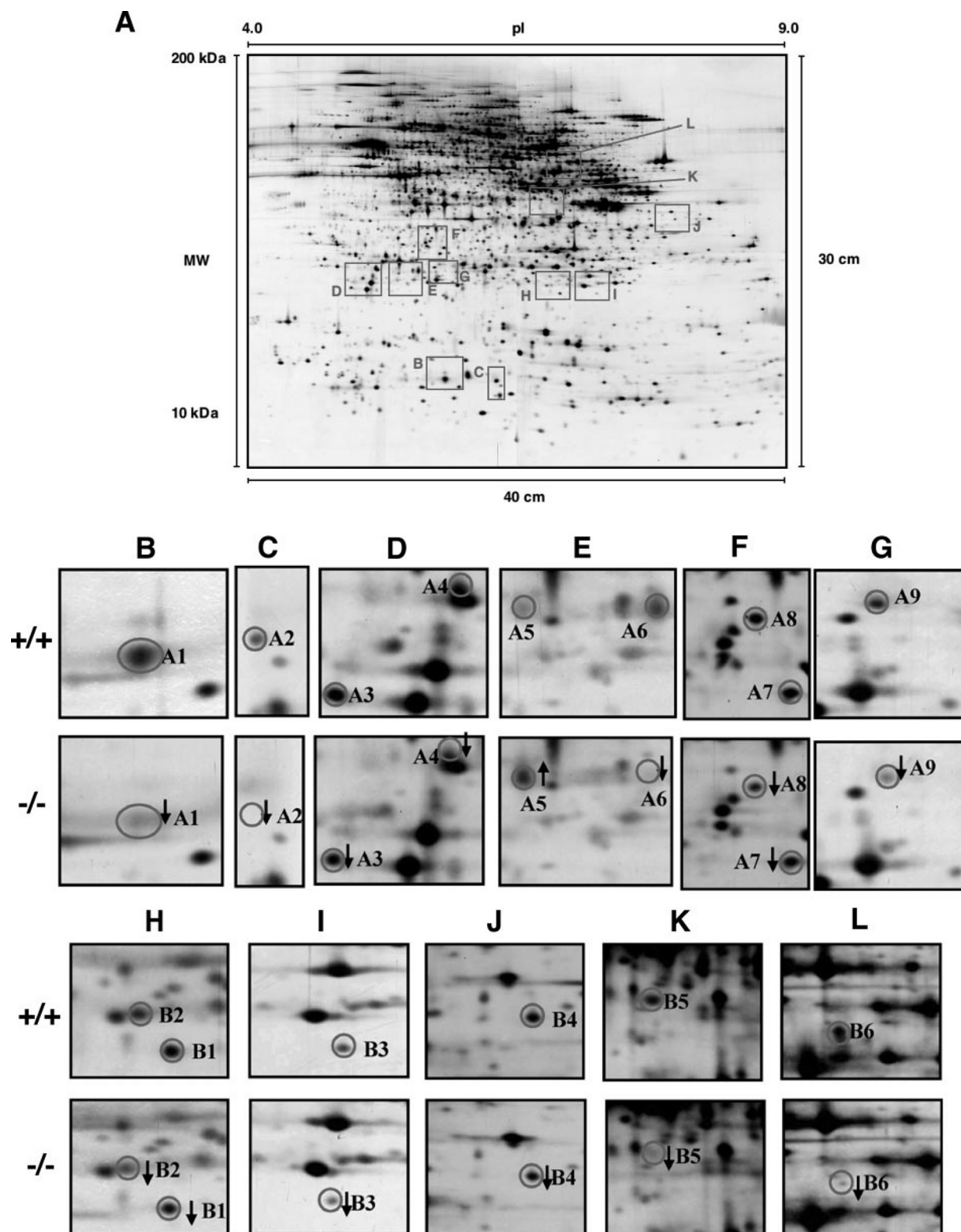


FIG. 1. Large-gel two-dimensional electrophoresis of the ventral midbrain proteome. A, representative two-dimensional electrophoresis of homogenates of the ventral midbrain of wild-type mice. Visual inspection of the gel allows identification of ~8,000 discrete protein spots. B–L, analysis of *parkin*^{-/-} ($n = 10$) and wild-type ($n = 10$) samples reveals consistent changes in the intensity of 15 protein spots with 14 protein spots showing decreased staining intensity and 1 showing increased staining in *parkin*^{-/-} mice. Protein spots showing consistent alterations in intensity are identified with an alphanumeric code.

phosphate-buffered saline followed by 10 ml of fresh 2.5% glutaraldehyde plus 2.5% formaldehyde in 100 mM cacodylate buffer. Brains were removed and post-fixed in the above fixative for an additional 18 h at 4 °C. Brains were washed in phosphate-buffered saline and cut into 1-mm thick coronal sections, and striata were dissected and processed for standard electron microscopy by epon embedding with osmium

tetroxide fixation and uranyl acetate counterstaining. Mitochondrial number and morphology were determined in images from 2–5 different fields from 2 mice per genotype by an investigator blind to the genotype.

Body Weight Measurements—Body weights were measured in *parkin*^{-/-} and wild-type mice at regular intervals beginning 10 days after weaning. Weights were analyzed by two-way analysis of variance fol-

TABLE I
Protein alterations in *parkin*^{-/-} mice

Protein	Spot number	Accession number ^a	Frequency of alteration ^b	Quantitative changes ^c
				%
Proteins involved in mitochondrial OXPHOS				
Pyruvate dehydrogenase E1 α 1	B6	P35487	7	-57.2 \pm 15.4
NADH-ubiquinone oxidoreductase 24-kDa subunit	A5	Q9D6J6	7	+41.4 \pm 10.9
NADH-ubiquinone oxidoreductase 24-kDa subunit	A6	Q9D6J6	7	-27.8 \pm 11.4
NADH-ubiquinone oxidoreductase 30-kDa subunit	A7	Q9DCT2	8	-9.1 \pm 2.4
Cytochrome c oxidase, subunit Vb	A2	P12075	7	-48.7 \pm 11.7
Proteins involved in oxidative stress				
Peroxiredoxin 2	A3	Q61171	8	-26.8 \pm 7.4
Peroxiredoxin 6	A9	O08709	6	-28.6 \pm 8.8
Peroxiredoxin 1	B2	P35700	8	-27 \pm 5.1
Lactylglutathione lyase	A4	Q9CPU0	9	-20.0 \pm 4.7
Other Proteins				
Profilin II	A1	Q9JJV2	7	-24.2 \pm 8.0
Hypothetical protein dJ37E16.5 (novel protein similar to nitrophenylphosphatases from various organisms)	A8	Q9UGY2	8	-22.0 \pm 8.1
Vacuolar protein sorting-29	B1	Q9QZ88	6	-13.0 \pm 1.9
α -Crystallin, chain B	B3	P23927	7	-27.6 \pm 6.5
Heterogeneous nuclear ribonucleoprotein A1	B4	P49312	9	-14.6 \pm 4.6
Lasp-1	B5	Q61792	7	-49.3 \pm 13.2

^a SWISS-PROT/TrEMBL accession number.

^b Number of pairs of mice showing consistent alterations in *parkin*^{-/-} mice.

^c Percentage changes shown as the mean \pm S.E. All alterations are statistically significant by Student's *t* test (*p* < 0.05).

lowed by Bonferroni post-hoc analysis. Data for adult male mice were collected in conjunction with behavioral analysis and were analyzed by unpaired Student's *t* test.

Serum Antioxidant Capacity Assay—Mice were fasted overnight to minimize variability due to dietary uptake. Mice were euthanized by CO₂ inhalation, blood was collected in heparinized tubes, and serum was isolated by centrifugation at 1200 rpm for 10 min. Serum total antioxidant capacity was measured by the conversion of Cu²⁺ to Cu¹⁺ using a colorimetric assay and is represented as μ M uric acid equivalents and carried out as per manufacturer's instructions (Total Antioxidant Potential, Oxis Research). Data were analyzed by unpaired Student's *t* test.

Protein Carbonyl Assay—Brains were homogenized in 50 mM Tris, 150 mM NaCl, and 1% v/v Triton X-100, pH 7.5, and insoluble material was removed by centrifugation. Supernatants were assayed for protein content (BCA, Pierce) and 20 μ g of protein was assayed for protein carbonyls as per the manufacturer's instructions (OxyBlot, Chemicon). Briefly, proteins were diluted into a final concentration of 6% SDS and reacted with 2,4-dinitrophenylhydrazine for 15 min. After the reaction, samples were neutralized, electrophoresed on NuPage gels (Invitrogen), transferred to nitrocellulose (Protran BA-83, Schleicher & Schuell), and Western-blotted using an antibody specific to the dinitrophenylhydrazine-derivatized residues on oxidatively damaged proteins. Blots were stripped and subsequently reprobbed for actin (AC-15, Abcam, Cambridge, MA) to confirm equivalent protein loading.

Immunohistochemistry—Brains were removed, fixed in neutral-buffered formalin for 2 h at room temperature, paraffin-embedded, and sectioned as previously described (24). Tissue sections were blocked with 10% goat serum, incubated with an antibody to Michael adducts of 4HNE (#393207, 1:200, Calbiochem) and then with an avidin-conjugated secondary. Immunoreactivity was visualized with diaminobenzidine.

RESULTS

Proteomic Analysis of *parkin*^{-/-} Mice—Because *parkin* is an E3 ubiquitin ligase (26), we anticipated that loss of *parkin* would result in accumulation of its substrates, which may in turn cause nigrostriatal dysfunction and nigral degeneration. To identify the proteomic difference between *parkin*^{-/-} and wild-type mice, we used large-gel two-dimensional electrophoresis (34) to separate proteins in the ventral midbrain of each of the 10 pairs of *parkin*^{-/-} and wild-type mice at ~8 months of age. Proteins were resolved in the first dimension by their isoelectric point (pI) on a 40-cm tube gel using carrier ampholytes and subsequently resolved in the second dimension by their molecular weight on 40 \times 30-cm SDS-PAGE gels. After silver staining, we detected reproducible, specific changes in 15

of ~8000 discrete spots between the genotypes (Fig. 1). Contrary to our expectations, the staining intensity of all but one of these 15 protein spots was decreased in *parkin*^{-/-} mice. Isolation of protein spots from these gels followed by trypsin digestion and subsequent matrix-assisted laser desorption ionization and electrospray ionization MS provided the identification of these proteins (Table I). Fourteen of the 15 spots represented distinct proteins, whereas one protein was detected twice in 2 adjacent spots (A5 and A6) with varying pI, suggesting a post-translational modification. Changes in protein spot intensity that were confirmed in more than six pairs of *parkin*^{-/-} and wild-type mice were scored (Table I).

The majority of the proteins altered in *parkin*^{-/-} mice are functionally implicated in either mitochondrial respiration (subunits of pyruvate dehydrogenase and mitochondrial complexes I and IV) or oxidative stress (peroxiredoxin (PRDX) 1, 2, and 6 and lactylglutathione lyase), indicating a connection between loss of *parkin* expression and mitochondrial and/or antioxidant deficiencies. The 24-kDa subunit of complex I was shifted to a more acidic pI in the *parkin*^{-/-} brain (Fig. 1E, spots A5 and A6), indicating the protein had undergone a differential post-translational modification in the *parkin*^{-/-} mouse brain. Based on the nature and degree of the pI shift from spot A6 to A5, possible modifications included oxidation or nitration of the protein. These modifications have been shown previously to appear in cells and tissues after exposure to oxidative stress (36–38). The alteration of both 24- and 30-kDa subunits suggested a general impairment of complex I in *parkin*^{-/-} mice. Furthermore, spot B1 (subunit Vb of complex IV) was also down-regulated in *parkin*^{-/-} mice, suggesting additional alterations in complex IV of the mitochondrial respiratory chain. The remaining proteins include those regulating the cytoskeleton (profilin II and lasp-1), vesicular transport (vacuolar protein sorting-29), and inhibiting aggregation of misfolded proteins (α -crystallin).

***parkin*^{-/-} Mice Exhibit Reduced Mitochondrial Respiration**—Previous reports suggest that PD may be linked to mitochondrial dysfunction (39). The biochemical changes detected in mitochondrial markers in the ventral midbrain of *parkin*^{-/-} mice (Fig. 1) suggested possible mitochondrial deficiency in these mice. To address this issue directly, we examined the metabolic capacity of mitochondria isolated from the striatum

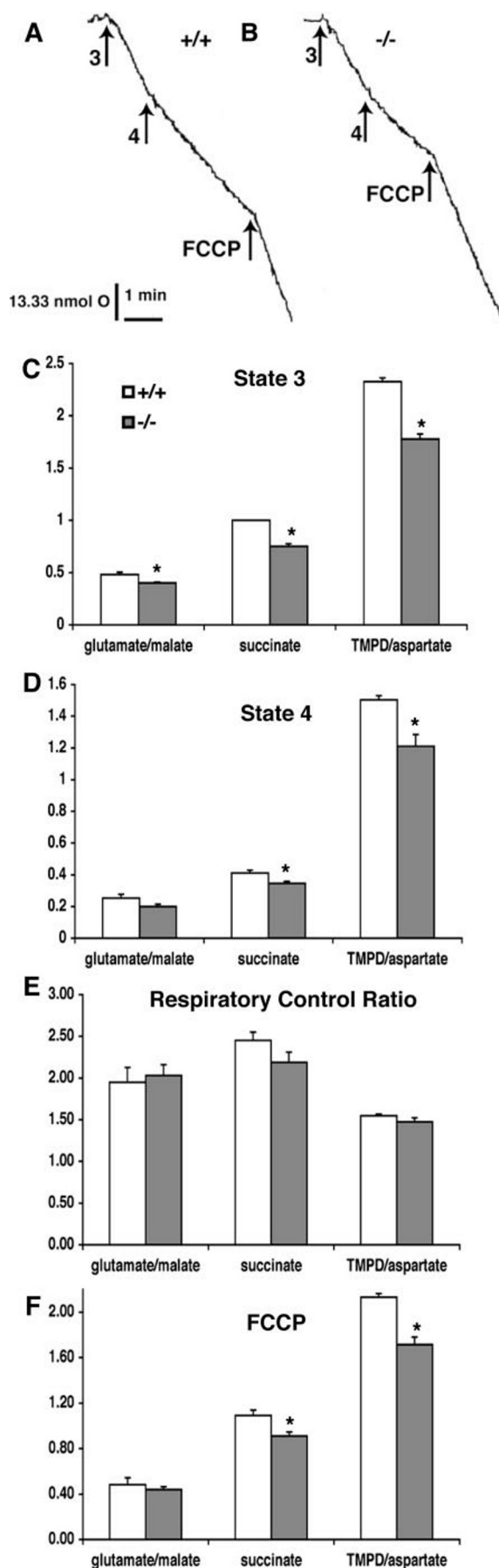


FIG. 2. Impaired mitochondrial function in *parkin*^{-/-} mice. *A* and *B*, representative traces of respiration rates in the mitochondria isolated from the striatum of wild-type (*A*) and *parkin*^{-/-} mice (*B*).

of *parkin*^{-/-} mice and wild-type controls by assaying for state 3 and state 4 respiration using substrates for complex I (glutamate/malate), complex II (succinate), and complex III/IV (TMPD/ascorbate). State 3 respiration measures the capacity of mitochondria to metabolize oxygen and the selected substrate in the presence of a limiting quantity of ADP, which is a substrate for complex V, the ATP synthase. In contrast, state 4 respiration occurs when all ADP is exhausted and measures respiration associated with proton leak across the inner mitochondrial membrane and represents a “basal-coupled” rate of respiration for each metabolic substrate.

Consistent with reductions in several units of complexes I and IV, we observed reduced rates of State 3 respiration (wild type versus *parkin*^{-/-}: 75.6 ± 13.1 versus 62.8 ± 11.2 , 147.7 ± 17.3 versus 110.3 ± 11.1 , and 366.6 ± 72.2 versus 282.2 ± 59.7 nmol of O₂/min/mg of protein for complex I, II, and III/IV, respectively; data are the mean \pm S.E.), indicating a reduced capacity of mitochondrial metabolism. Representative traces for succinate-mediated respiration are shown in Fig. 2, *A* and *B*. Due to intra-day variations in absolute respiratory rate, data were analyzed as a fraction of the wild-type state 3 respiration for succinate (Fig. 2*C*). Consistent, statistically significant reductions were seen in mitochondria from *parkin*^{-/-} mice using substrates that enter the electron transport chain at complex I (glutamate/malate), complex II (succinate), and complex III/IV (TMPD/ascorbate), suggesting an overall reduction in respiratory capacity. Measurement of state 4 respiration using either succinate or TMPD/ascorbate similarly exhibited a significant decrease in capacity in *parkin*^{-/-} mice (Fig. 2*D*). The comparable magnitude of reduction in both state 3 and 4 respiration further supported the indication of reduced mitochondrial capacity for electron transport in *parkin*^{-/-} mice.

Respiratory control ratio (ratio of state 3:state 4 respiration) provides a measure of the efficiency of coupling of the electron transport chain. The respiratory control ratio (Fig. 2*E*) for all substrates was similar in *parkin*^{-/-} and wild-type mice, indicating that the relative efficiency of metabolic coupling between the complexes of the electron transport chain is unchanged. The absence of a change in the respiratory control ratio indicates that the decrease in metabolism was likely due to a reduction in capacity (rather than efficiency) of the electron transport chain.

A reduction in electron transport chain capacity is further confirmed by the significant reduction in respiratory rate for both succinate and TMPD/ascorbate after treatment with FCCP (Fig. 2*F*). FCCP treatment results in a collapse of the proton gradient across the inner mitochondrial membrane and allows mitochondrial respiration to proceed at the maximal capacity for the components of the electron transport chain without regard for either the capacity of complex V or proton leak. Thus, the decrease in mitochondrial respiration can be linked to a decrease in the capacity of the electron transport chain rather than a defect in ATP synthase capacity or function.

Mitochondrial Dysfunction Is Not Coupled with Alterations in Mitochondrial Morphology—The decreased abundance of

Vertical arrows indicate state 3, state 4, and FCCP respiration. *C* and *D*, analysis of mitochondria from 5 pairs of samples (striata from 2 mice were pooled for each sample) reveals a statistically significant decrease in capacity for state 3 (*C*) or state 4 (*D*) respiration for all electron transport substrates tested. *, $p < 0.05$ (Student's *t* test). *E*, unaltered respiratory control ratio in *parkin*^{-/-} mitochondria, indicating normal efficiency of electron transport. *F*, following treatment with FCCP, mitochondria from *parkin*^{-/-} mice exhibit significant reductions in uncoupled respiratory rates with succinate or TMPD/ascorbate substrates, indicating a reduced capacity of the electron transport chain. *, $p < 0.05$ (Student's *t* test)

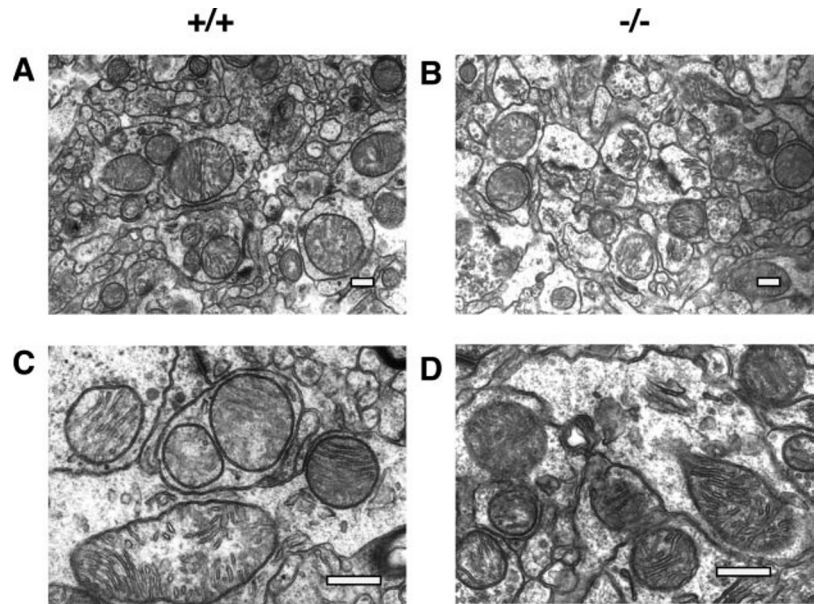


FIG. 3. Normal gross morphology of mitochondria in the striatum of *parkin*^{-/-} mice. A and B, electron microscopy analysis (20,000 \times) reveals well formed membranes and clearly discernible cristae in the mitochondria of the wild-type (A) and *parkin*^{-/-} (B) striatum. C and D, higher power views (40,000 \times) confirm normal gross morphology of wild-type (C) and *parkin*^{-/-} (D) mitochondria. Scale bar, 200 nm.

several mitochondrial proteins and the altered mitochondrial respiratory chain activity prompted us to examine the morphology of striatal mitochondria from *parkin*^{-/-} mice and wild-type controls. Previous studies indicate that *parkin*-null flies exhibit morphological changes in mitochondria of the wing muscle and spermatocytes (33). Electron microscopy of striatal sections revealed no apparent change in the total number or size of mitochondria present in *parkin*^{-/-} mice (data not shown). Examination of 100 μm^2 of striatal area from two mice per genotype showed no gross alterations in mitochondrial morphology in *parkin*^{-/-} mice (Fig. 3, A and B). Further examination at higher magnification (40,000 \times) showed that both *parkin*^{-/-} and wild-type mitochondria had well formed cristae with no apparent swelling or separation of the inner and outer membranes (Fig. 3, C and D). These results suggest that reduced mitochondrial respiratory chain activity was not associated with detectable morphological changes in the mitochondria of *parkin*^{-/-} mice.

***parkin*^{-/-} Mice Exhibit Reduced Body Weight Gain**—To determine whether the reduced mitochondrial respiratory capacity in the *parkin*^{-/-} mouse results in a broad alteration in metabolic activity, we examined early weight gain in *parkin*^{-/-} mice during the period immediately after weaning. Mice that were weaned at \sim 20 days of age were monitored for weight gain starting at \sim 30 days of age. Animals were weighed regularly for an additional 3 months. Data were pooled in either 10- or 20-day bins (\pm 2 days). Over the course of the measurements, both male and female *parkin*^{-/-} mice exhibited a significant decrease in the rate and total amount of weight gain (Fig. 4, A and B). Adult (6–12-month-old) male *parkin*^{-/-} mice also exhibited significantly lower body weights (Fig. 4C).

Reduced Antioxidant Capacity and Elevated Oxidative Damage in *parkin*^{-/-} Mice—The mitochondrial respiratory dysfunction in *parkin*^{-/-} mice prompted us to investigate whether increased levels of oxidation products could be detected in these mice. Three of the proteins identified in our proteomic screen to be decreased in *parkin*^{-/-} mice were small peroxide reductases, suggesting that the *parkin*^{-/-} mouse may have a reduced ability to respond to the generation of ROS. Analysis of serum total antioxidant potential, defined as copper reducing equivalents, revealed that *parkin*^{-/-} mice ($n = 12$) had reduced antioxidant capacity as compared with age-matched wild-type mice ($n = 13$) (5–12 months of age) (Fig. 5A).

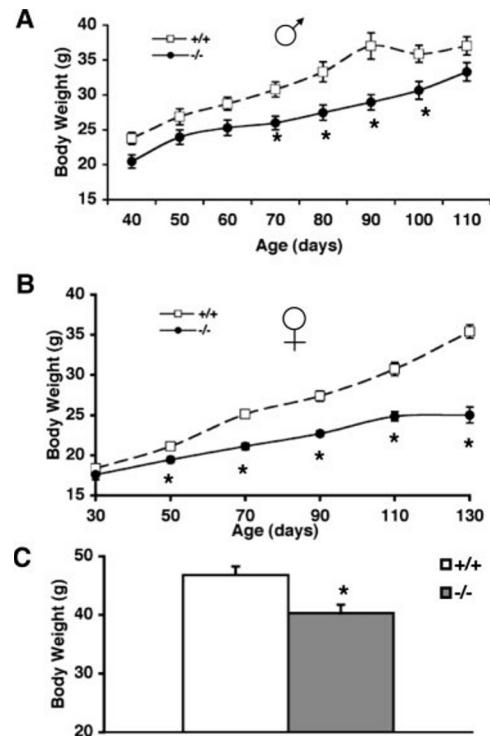


FIG. 4. Reduced body weight of *parkin*^{-/-} mice. A and B, *parkin*^{-/-} mice exhibit a significantly reduced rate of weight gain over the course of the study (analysis of variance $p < 0.001$) (A, males; B, females). Post-hoc analysis of male body weights at the various time points shows that *parkin*^{-/-} mice ($n = 4-8$) are significantly smaller than wild-type controls ($n = 5-13$) between the ages of 70 and 100 days (*, Bonferroni, $p < 0.05$). Post-hoc analysis of female body weights at the various time points shows that *parkin*^{-/-} mice ($n = 6-32$) are significantly smaller than wild-type controls ($n = 3-9$) at all ages (*, Bonferroni, $p < 0.001$) except the initial measurement at 30 days of age. C, subsequent analysis of a large cohort of adult male mice (6–12 months) shows that *parkin*^{-/-} mice ($n = 25$) still exhibit significantly reduced body weight compared with age-matched wild-type mice ($n = 20$). *, $p < 0.05$ (Student's t test).

We then examined *parkin*^{-/-} and wild-type brains for protein and lipid byproducts modified by ROS. Analysis of brain lysates of *parkin*^{-/-} and wild-type mice at 3 and 18–20 months revealed elevated levels of protein carbonyls, a general marker of oxidative damage, in aged (18–20 months) *parkin*^{-/-} mice but

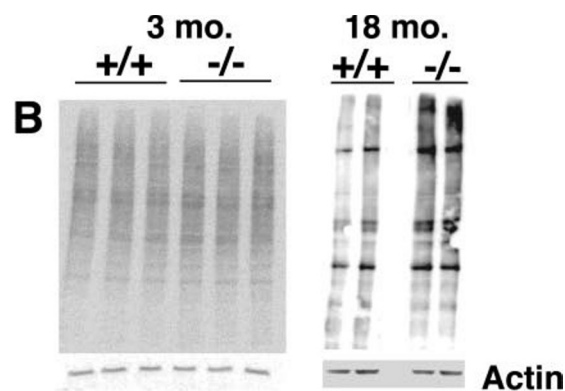
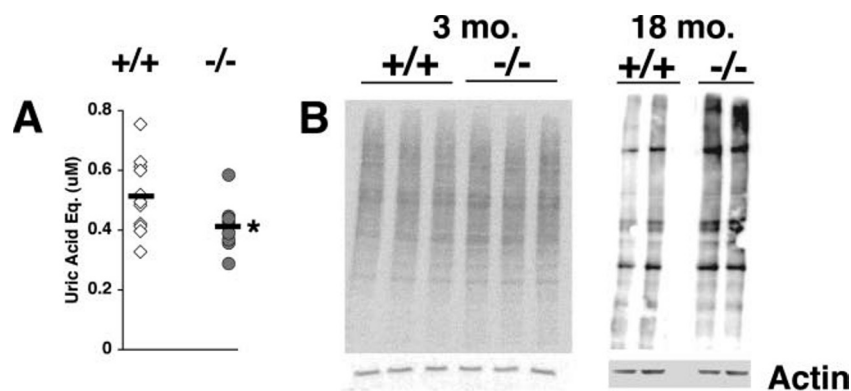
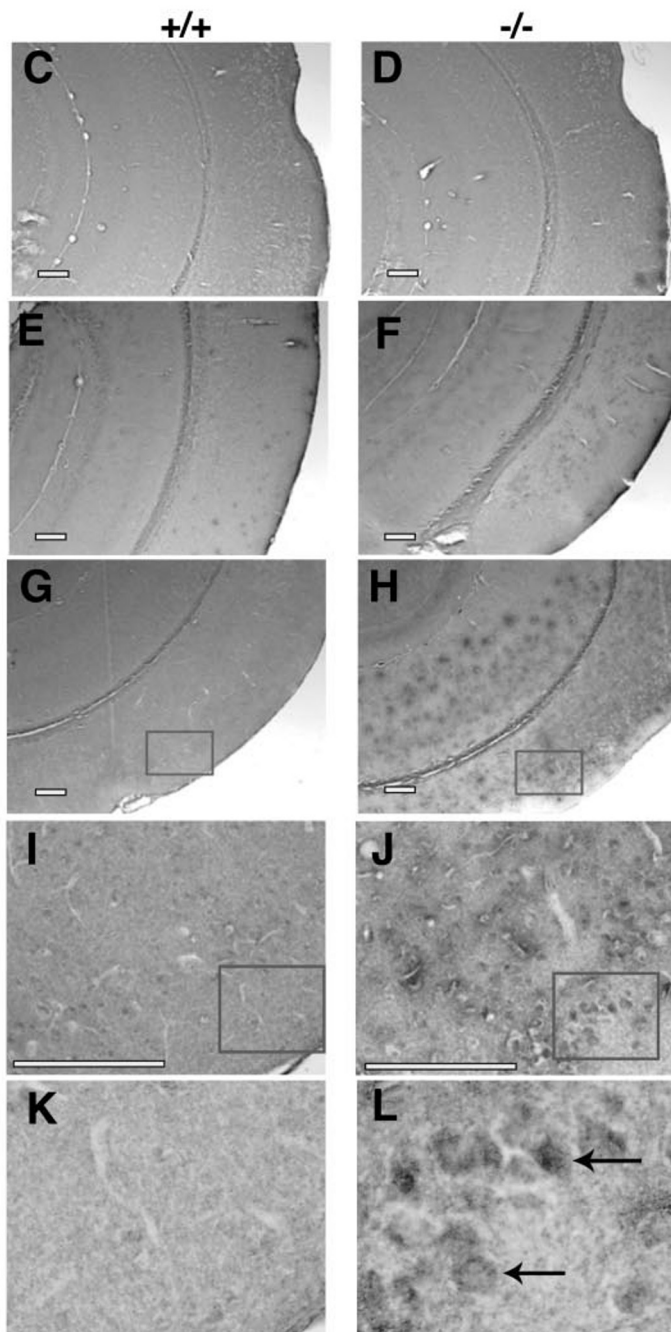


FIG. 5. Reduced antioxidant capacity and increased ROS damage in *parkin*^{-/-} mice. *A*, assays for serum antioxidant potential reveals a significant decrease in the total reducing capacity of *parkin*^{-/-} mice ($n = 12$), as compared with wild-type mice ($n = 13$). *, $p < 0.01$ (Student's t test). *B*, analysis of brain lysates from *parkin*^{-/-} and wild-type mice at 3 and 18–20 months reveals that aged (18–20 month) *parkin*^{-/-} mice exhibit increased levels of protein carbonyls. Incubation of the same blots with anti-actin antibody confirms equivalent loading of proteins in each lane. *C–J*, immunohistochemical analysis of *parkin*^{-/-} and wild-type mice reveals an age-dependent increase in 4HNE immunoreactivity in the *parkin*^{-/-} brain (*D*, *F*, and *H*) as compared with age-matched wild-type mice (*C*, *E*, and *G*). Comparable coronal sections of *parkin*^{-/-} and control brains at 3 (*C* and *D*), 6 (*E* and *F*), and 18 (*G* and *H*) months of age are shown. *I–L*, higher power views of the boxed areas in *G* and *H* (*I* and *J*) or the boxed areas in *I* and *J* (*K* and *L*) show increased 4HNE immunoreactivity in *parkin*^{-/-} mice (*J* and *L*). Arrows indicate 4HNE immunoreactivity in cell bodies. Scale bar, 200 μm .



not in young (3 month) *parkin*^{-/-} mice relative to the control ($n = 3$ and 2 per genotype at 3 and 18–20 months, respectively) (Fig. 5B).

Several lipid peroxides, especially 4HNE, are highly reac-

tive, avidly form adducts with many proteins and have been detected in Lewy bodies (40). Immunohistochemical analysis of *parkin*^{-/-} and wild-type mice at 3, 6, and 18 months revealed age-dependent increases in 4HNE immunoreactivity in the

brain of *parkin*^{-/-} mice as compared with wild-type controls (Fig. 5, C–L). At 3 months of age, neither *parkin*^{-/-} nor wild-type mice showed significant immunoreactivity for 4HNE (Fig. 5, C and D). At 6 months, modest 4HNE immunoreactivity was detectable in brains of both *parkin*^{-/-} and wild-type mice (Fig. 5, E and F). By 18 months, *parkin*^{-/-} brains exhibit a marked increase in 4HNE immunoreactivity (Fig. 5, G–L). Higher magnification images show staining in cell bodies (Fig. 5L, arrows) in the *parkin*^{-/-} brain. These findings demonstrated that, over the course of 18 months, *parkin*^{-/-} animals experienced an increased incidence of ROS-mediated damage as compared with age-matched wild-type animals.

DISCUSSION

The identification of several genes linked to familial PD has provided new venues for the investigation of the mechanism underlying the selective nigral degeneration. The first gene linked to familial PD was α -synuclein, in which missense and triplication mutations have been reported (41–43). The linkage of α -synuclein mutations to PD and the accumulation of insoluble α -synuclein in Lewy bodies provided a strong link between protein aggregation and PD pathogenesis. Similarly, mutations in parkin and UCHL-1, two proteins linked to the ubiquitin-proteasome pathway, supported a possible involvement of aberrant accumulation of insoluble protein substrate(s) in PD pathogenesis. However, most *parkin*-linked PD cases lack Lewy bodies, suggesting that parkin mutations may cause PD by mechanisms distinct from protein aggregation and Lewy body formation (22, 23). The association of parkin expression with cytoprotection in cultured cells (29) and flies (44), and its amelioration of mitochondrial dysfunction-induced cell death (31), provided tantalizing clues to an alternative mode of action, namely a regulatory function for parkin in mitochondrial activity.

In the present study we compared the proteome of the ventral midbrain of *parkin*^{-/-} and wild-type mice and found specific and consistent decreases in the steady-state abundance of 13 proteins and altered electrophoretic mobility of 1 additional protein. Eight of these proteins are linked to mitochondrial respiration or detoxification of byproducts of mitochondrial respiration. Four proteins that are specifically reduced, *i.e.* the E1 α subunit of pyruvate dehydrogenase, the 24- and 30-kDa subunits of complex I and subunit Vb of complex IV, are all directly involved in mitochondrial oxidative phosphorylation activity. An additional one, lactylglutathione lyase, is part of a two-step enzymatic cascade to metabolize methylglyoxal to lactate (45, 46). Methylglyoxal is the non-enzymatic breakdown product of glycerol 3-phosphate and is linked to formation of advanced glycation end products. Accumulations of advanced glycation end product-modified proteins are present in Lewy bodies of PD patients (47). Three additional proteins showing selective and reproducible reductions, PRDX 1, 2, and 6, are small, thiol-dependent peroxidases. Members of the PRDX family have been linked to protection from ROS stresses, and mouse models of loss of PRDX proteins result in enhanced sensitivity to oxidative stress (48–50).

The decreased steady-state levels of proteins essential for mitochondrial respiratory chain activity are accompanied by measurable physiological changes in mitochondria from brains of *parkin*^{-/-} mice. These alterations resulted in reduced electron transport chain capacity in mitochondria from *parkin*^{-/-} mice and were analogous to functional alterations described in mitochondria isolated from PD patients (51). Furthermore, studies have shown that overexpression of α -synuclein induces decreases in mitochondrial respiration and increases sensitivity to mitochondrial stress (52–54), providing further support for a common mitochondrial mechanism in the pathogenesis of PD. Coupled to these mitochondrial changes were decreased

levels of three antioxidant proteins and one protein linked to detoxifying mitochondrial glycation byproducts along with an overall reduction in serum antioxidant capacity. Others have reported lower levels of reduced glutathione in another *parkin*^{-/-} mouse model (25), analogous to changes seen in PD patients (55). In similar experiments, overexpression of mutant parkin results in increased markers of oxidative stress (32). These decreases in antioxidant capacity are likely to render *parkin*^{-/-} mice more susceptible to ROS-mediated damage.

In addition to decreases in several proteins linked to mitochondria and ROS, levels of several other proteins with possible connections to PD pathology were decreased in *parkin*^{-/-} mice. The small chaperone protein, α -crystallin, regulates the stability of and inhibits aggregation of proteins in many tissues, notably the lens of the eye (56). Vacuolar protein sorting-29 is a mammalian homolog of a yeast protein linked to protein sorting and trafficking between the endoplasmic reticulum/Golgi and the endosome (57) and, thus, may be involved in the synaptic transmission changes we have previously observed in the *parkin*^{-/-} mice. Lasp1 is a molecular scaffold protein that has been associated with process extension (58), and may be involved in the regulation of synapse maintenance. Similarly, profilin II is a small, actin-binding protein that has been shown to negatively regulate neurite formation, suggesting a role in the formation and maintenance of synapses (59). Finally, heterogeneous nuclear ribonucleoprotein A1 is a component of an RNA binding complex that regulates RNA splicing (60) and may be functionally related to the p38 subunit of tRNA synthase, a substrate for parkin-mediated ubiquitylation (61).

Consistent with increased susceptibility to ROS damage, we detected elevated levels of oxidized proteins and lipids in the brains of *parkin*^{-/-} mice. Increases in 4HNE immunoreactive species are present in Lewy bodies of PD brains (40). Furthermore, *in vitro* data indicates that 4HNE forms adducts with, and inhibits the function of the D1 receptor and DAT (16, 17), providing a functional correlation between ROS damage and decreases in DA signaling in PD. This may suggest a connection between the mitochondrial dysfunction and our findings of increased extracellular DA in the striatum of *parkin*^{-/-} mice. Elevated extracellular DA has been shown to create an oxidizing environment both *in vitro* and *in vivo* (62, 63). This environment results in ROS damage and mitochondrial dysfunction analogous to our findings (64). Oxidative damage to lipids may result in increased lipid peroxides, including 4HNE. These labile lipid peroxides may damage DAT, resulting in reduced DAT activity (17), leading to elevated extracellular DA, thereby exacerbating the oxidative stress. A recent paper shows that parkin is inactivated by ROS (65), suggesting that increased ROS mediated damage may result in further decreases of parkin activity in PD brains. Clinical reports indicate that heterozygous parkin mutations may represent a risk factor for late-onset PD in a subset of cohorts (66). This presents the hypothetical scenario of a vicious cycle where decreased levels of parkin result in mitochondrial dysfunction, which in turn lead to increased ROS formation and further inactivation of parkin and so forth. Our data provide compelling evidence for mitochondrial dysfunction and oxidative stress in the absence of nigral degeneration. This suggests that these events may be proximal in the cascade of the pathogenesis of both idiopathic and parkin-linked familial PD.

Acknowledgments—We thank Andrea Martins, Bettina Esch, Mary Wines, and Xiaoyan Sun for assistance.

REFERENCES

1. Olanow, C. W., and Tatton, W. G. (1999) *Annu. Rev. Neurosci.* **22**, 123–144
2. Beal, M. F. (2003) *Ann. N. Y. Acad. Sci.* **991**, 120–131
3. Kosel, S., Hofhaus, G., Maassen, A., Vieregge, P., and Graeber, M. B. (1999) *Biol. Chem.* **380**, 865–870

4. Jenner, P., and Olanow, C. W. (1996) *Neurology* **47**, Suppl. 3, 5161–5170
5. Zhang, Y., Dawson, V. L., and Dawson, T. M. (2000) *Neurobiol. Dis.* **7**, 240–250
6. Schapira, A. H. (1998) *Biochim. Biophys. Acta* **1366**, 225–233
7. Dexter, D. T., Sian, J., Rose, S., Hindmarsh, J. G., Mann, V. M., Cooper, J. M., Wells, F. R., Daniel, S. E., Lees, A. J., Schapira, A. H. V., Jenner, P., and Marsden, C. D. (1994) *Ann. Neurol.* **35**, 38–44
8. Langston, J. W., Ballard, P., Tetrud, J. W., and Irwin, I. (1983) *Science* **219**, 979–980
9. Koller, W. C. (1986) *Neurology* **36**, 1147
10. Singer, T. P., Ramsay, R. R., McKeown, K., Trevor, A., and Castagnoli, N. E., Jr. (1988) *Toxicology* **49**, 17–23
11. Sherer, T. B., Betarbet, R., Stout, A. K., Lund, S., Baptista, M., Panov, A. V., Cookson, M. R., and Greenamyre, J. T. (2002) *J. Neurosci.* **22**, 7006–7015
12. Sousa, S. C., Maciel, E. N., Vercesi, A. E., and Castilho, R. F. (2003) *FEBS Lett.* **543**, 179–183
13. Schmuck, G., Rohrdanz, E., Tran-Thi, Q. H., Kahl, R., and Schluter, G. (2002) *Neurotox. Res.* **4**, 1–13
14. Alam, Z. I., Daniel, S. E., Lees, A. J., Marsden, D. C., Jenner, P., and Halliwell, B. (1997) *J. Neurochem.* **69**, 1326–1329
15. Yoritaka, A., Hattori, N., Uchida, K., Tanaka, M., Stadtman, E. R., and Mizuno, Y. (1996) *Proc. Natl. Acad. Sci. U. S. A.* **93**, 2696–2701
16. Shin, Y., White, B. H., Uh, M., and Sidhu, A. (2003) *Brain Res.* **968**, 102–113
17. Morel, P., Tallineau, C., Pontcharraud, R., Piriou, A., and Huguot, F. (1998) *Neurochem. Int.* **33**, 531–540
18. Chun, H. S., Gibson, G. E., DeGiorgio, L. A., Zhang, H., Kidd, V. J., and Son, J. H. (2001) *J. Neurochem.* **76**, 1010–1021
19. Dawson, T. M., and Dawson, V. L. (2003) *Science* **302**, 819–822
20. Vaughan, J. R., Davis, M. B., and Wood, N. W. (2001) *Ann. Hum. Genet.* **65**, 111–126
21. Kitada, T., Asakawa, S., Hattori, N., Yamamura, Y., Minoshima, S., Yokochi, M., Mizuno, Y., and Shimizu, N. (1998) *Nature* **392**, 605–608
22. Farrer, M., Chan, P., Chen, R., Tan, L., Lincoln, S., Hernandez, D., Forno, L., Gwinn-Hardy, K., Petrucelli, L., Hussey, J., Singleton, A., Tanner, C., Hardy, J., and Langston, J. W. (2001) *Ann. Neurol.* **50**, 293–300
23. Hayashi, S., Wakabayashi, K., Ishikawa, A., Nagai, H., Saito, M., Maruyama, M., Takahashi, T., Ozawa, T., Tsuji, S., and Takahashi, H. (2000) *Movement Disorders* **15**, 884–888
24. Goldberg, M. S., Fleming, S. M., Palacino, J. J., Cepeda, C., Lam, H. A., Bhatnagar, A., Meloni, E. G., Wu, N., Ackerson, L. C., Klapstein, G. J., Gajendiran, M., Roth, B. L., Chesselet, M. F., Maidment, N. T., Levine, M. S., and Shen, J. (2003) *J. Biol. Chem.* **278**, 43628–43635
25. Itier, J. M., Ibanez, P., Mena, M. A., Abbas, N., Cohen-Salmon, C., Bohme, G. A., Laville, M., Pratt, J., Corti, O., Pradier, L., Ret, G., Joubert, C., Periquet, M., Araujo, F., Negroni, J., Casarejos, M. J., Canals, S., Solano, R., Serrano, A., Gallego, E., Sanchez, M., Deneffe, P., Benavides, J., Tremp, G., Rooney, T. A., Brice, A., and De Yebenes, J. G. (2003) *Hum. Mol. Genet.* **12**, 2277–2291
26. Shimura, H., Hattori, N., Kubo, S., Mizuno, Y., Asakawa, S., Minoshima, S., Shimizu, N., Iwai, K., Chiba, T., Tanaka, K., and Suzuki, T. (2000) *Nat. Genet.* **25**, 302–305
27. Cookson, M. R. (2003) *Neuromolecular Med.* **3**, 1–13
28. Xu, J., Kao, S. Y., Lee, F. J., Song, W., Jin, L. W., and Yankner, B. A. (2002) *Nat. Med.* **8**, 600–606
29. Petrucelli, L., O'Farrell, C., Lockhart, P. J., Baptista, M., Kehoe, K., Vink, L., Choi, P., Wolozin, B., Farrer, M., Hardy, J., and Cookson, M. R. (2002) *Neuron* **36**, 1007–1019
30. Staropoli, J. F., McDermott, C., Martinat, C., Schulman, B., Demireva, E., and Abeliovich, A. (2003) *Neuron* **37**, 735–749
31. Darios, F., Corti, O., Lucking, C. B., Hampe, C., Muriel, M. P., Abbas, N., Gu, W. J., Hirsch, E. C., Rooney, T., Ruberg, M., and Brice, A. (2003) *Hum. Mol. Genet.* **12**, 517–526
32. Hyun, D. H., Lee, M., Hattori, N., Kubo, S., Mizuno, Y., Halliwell, B., and Jenner, P. (2002) *J. Biol. Chem.* **277**, 28572–28577
33. Greene, J. C., Whitworth, A. J., Kuo, I., Andrews, L. A., Feany, M. B., and Pallanck, L. J. (2003) *Proc. Natl. Acad. Sci. U. S. A.* **100**, 4078–4083
34. Klose, J., Nock, C., Herrmann, M., Stuhler, K., Marcus, K., Bluggel, M., Krause, E., Schalkwyk, L. C., Rastan, S., Brown, S. D., Bussow, K., Himmelbauer, H., and Lehrach, H. (2002) *Nat. Genet.* **30**, 385–393
35. Klose, J. (1999) *Methods Mol. Biol.* **112**, 67–85
36. MacMillan-Crow, L. A., Crow, J. P., and Thompson, J. A. (1998) *Biochemistry* **37**, 1613–1622
37. Viner, R. I., Williams, T. D., and Schoneich, C. (1999) *Biochemistry* **38**, 12408–12415
38. Yang, K. S., Kang, S. W., Woo, H. A., Hwang, S. C., Chae, H. Z., Kim, K., and Rhee, S. G. (2002) *J. Biol. Chem.* **277**, 38029–38036
39. Greenamyre, J. T., MacKenzie, G., Peng, T. I., and Stephans, S. E. (1999) *Biochem. Soc. Symp.* **66**, 85–97
40. Castellani, R. J., Perry, G., Siedlak, S. L., Nunomura, A., Shimohama, S., Zhang, J., Montine, T., Sayre, L. M., and Smith, M. A. (2002) *Neurosci. Lett.* **319**, 25–28
41. Polymeropoulos, M. H., Lavedan, C., Leroy, E., Ide, S. E., Dehejia, A., Dutra, A., Pike, B., Root, H., Rubenstein, J., Boyer, R., Stenroos, E. S., Chandrasekharappa, S., Athanassiadou, A., Papapetropoulos, T., Johnson, W. G., Lazzarini, A. M., Duvoisin, R. C., Di Iorio, G., Golbe, L. I., and Nussbaum, R. L. (1997) *Science* **276**, 2045–2047
42. Zarranz, J. J., Alegre, J., Gomez-Esteban, J. C., Lezcano, E., Ros, R., Ampuero, I., Vidal, L., Hoenicka, J., Rodriguez, O., Atares, B., Llorens, V., Tortosa, E. G., del Ser, T., Munoz, D. G., and de Yebenes, J. G. (2004) *Ann. Neurol.* **55**, 164–173
43. Singleton, A. B., Farrer, M., Johnson, J., Singleton, A., Hague, S., Kachergus, J., Hulihan, M., Peuralinna, T., Dutra, A., Nussbaum, R., Lincoln, S., Crawley, A., Hanson, M., Maraganore, D., Adler, C., Cookson, M. R., Muentner, M., Baptista, M., Miller, D., Blacato, J., Hardy, J., and Gwinn-Hardy, K. (2003) *Science* **302**, 841
44. Yang, Y., Nishimura, I., Imai, Y., Takahashi, R., and Lu, B. (2003) *Neuron* **37**, 911–924
45. Cordeiro, C., and Freire, A. P. (1996) *Biochem. Soc. Trans.* **24**, 472S
46. Choudhary, D., Chandra, D., and Kale, R. K. (1997) *Toxicol. Lett.* **93**, 141–152
47. Munch, G., Luth, H. J., Wong, A., Arendt, T., Hirsch, E., Ravid, R., and Riederer, P. (2000) *J. Chem. Neuroanat.* **20**, 253–257
48. Lee, T. H., Kim, S. U., Yu, S. L., Kim, S. H., Park do, S., Moon, H. B., Dho, S. H., Kwon, K. S., Kwon, H. J., Han, Y. H., Jeong, S., Kang, S. W., Shin, H. S., Lee, K. K., Rhee, S. G., and Yu, D. Y. (2003) *Blood* **101**, 5033–5038
49. Neumann, C. A., Krause, D. S., Carman, C. V., Das, S., Dubey, D. P., Abraham, J. L., Bronson, R. T., Fujiwara, Y., Orkin, S. H., and Van Etten, R. A. (2003) *Nature* **424**, 561–565
50. Wang, X., Phelan, S. A., Forsman-Semb, K., Taylor, E. F., Petros, C., Brown, A., Lerner, C. P., and Paigen, B. (2003) *J. Biol. Chem.* **278**, 25179–25190
51. Sherer, T. B., Trimmer, P. A., Borland, K., Parks, J. K., Bennett, J. P., Jr., and Tuttle, J. B. (2001) *Brain Res.* **891**, 94–105
52. Hsu, L. J., Sagara, Y., Arroyo, A., Rockenstein, E., Sisk, A., Mallory, M., Wong, J., Takenouchi, T., Hashimoto, M., and Masliah, E. (2000) *Am. J. Pathol.* **157**, 401–410
53. Lee, H. J., Shin, S. Y., Choi, C., Lee, Y. H., and Lee, S. J. (2002) *J. Biol. Chem.* **277**, 5411–5417
54. Orth, M., Tabrizi, S. J., Schapira, A. H., and Cooper, J. M. (2003) *Neurosci. Lett.* **351**, 29–32
55. Serra, J. A., Dominguez, R. O., de Lustig, E. S., Guareschi, E. M., Famulari, A. L., Bartolome, E. L., and Marschoff, E. R. (2001) *J. Neural Transm.* **108**, 1135–1148
56. Dubin, R. A., Wawrousek, E. F., and Piatigorsky, J. (1989) *Mol. Cell. Biol.* **9**, 1083–1091
57. Haft, C. R., de la Luz Sierra, M., Bafford, R., Lesniak, M. A., Barr, V. A., and Taylor, S. I. (2000) *Mol. Biol. Cell* **11**, 4105–4116
58. Schreiber, V., Moog-Lutz, C., Regnier, C. H., Chenard, M. P., Boeuf, H., Vonesch, J. L., Tomasetto, C., and Rio, M. C. (1998) *Mol. Med.* **4**, 675–687
59. Da Silva, J. S., Medina, M., Zuliani, C., Di Nardo, A., Witke, W., and Dotti, C. G. (2003) *J. Cell Biol.* **162**, 1267–1279
60. Weighardt, F., Biamonti, G., and Riva, S. (1996) *Bioessays* **18**, 747–756
61. Corti, O., Hampe, C., Koutnikova, H., Darios, F., Jacquier, S., Prigent, A., Robinson, J. C., Pradier, L., Ruberg, M., Mirande, M., Hirsch, E., Rooney, T., Fournier, A., and Brice, A. (2003) *Hum. Mol. Genet.* **12**, 1427–1437
62. Gluck, M., Ehrhart, J., Jayatilleke, E., and Zeevalk, G. D. (2002) *J. Neurochem.* **82**, 66–74
63. Hastings, T. G., Lewis, D. A., and Zigmond, M. J. (1996) *Proc. Natl. Acad. Sci. U. S. A.* **93**, 1956–1961
64. Morikawa, N., Nakagawa-Hattori, Y., and Mizuno, Y. (1996) *J. Neurochem.* **66**, 1174–1181
65. Winklhofer, K. F., Henn, I. H., Kay-Jackson, P., Heller, U., and Tatzelt, J. (2003) *J. Biol. Chem.* **278**, 47199–47208
66. Foroud, T., Uniacke, S. K., Liu, L., Pankratz, N., Rudolph, A., Halter, C., Shults, C., Marder, K., Conneally, P. M., and Nichols, W. C. (2003) *Neurology* **60**, 796–801